A low-temperature structural phase transition in $CsPbF_3$

2001 J. Phys.: Condens. Matter 13 5077

(http://iopscience.iop.org/0953-8984/13/22/305)

INSTITUTE OF PHYSICS PUBLISHING JOURNAL OF PHYSICS: CONDENSED MATTER

J. Phys.: Condens. Matter **13** (2001) 5077–5088 www.iop.org/Journals/cm PII: S0953-8984(01)23233-0

A low-temperature structural phase transition in $CsPbF_3$

P Berastegui[1], S Hull[2,4] and S-G Eriksson[3]

[1] Department of Inorganic Chemistry, Stockholm University, S-106 91 Stockholm, Sweden
[2] The ISIS Facility, Rutherford Appleton Laboratory, Chilton, Didcot, Oxfordshire OX11 0QX, UK
[3] Studsvik Neutron Research Laboratory, S-611 82 Nyköping, Sweden

E-mail: s.hull@rl.ac.uk

Received 22 March 2001, in final form 20 April 2001

Abstract

The structural behaviour of caesium lead fluoride, $CsPbF_3$, has been investigated as a function of temperature in the range $148(2) \leqslant T$ (K) $\leqslant 276(2)$. The presence of a structural phase transition at ∼190 K reported from previous nuclear magnetic resonance measurements (Bouznik V M, Moskvich Yu N and Voronov V N 1976 *Chem. Phys. Lett.* **37** 464) has been confirmed by impedance spectroscopy and powder neutron diffraction studies. The former show that there is no significant discontinuity in the ionic conductivity σ at the transition temperature, only a change in the slope $\mathrm{d}\sigma/\mathrm{d}T$ at $T = 185(2)$ K. On cooling, the neutron diffraction data indicate a transition from the cubic perovskite structure ($Pm\bar{3}m$) to a rhombohedrally distorted perovskite arrangement (space group $R3c$) at $T = 187(5)$ K. The transition is discontinuous, with a small volume change $\Delta V/V \sim 0.113(7)\%$. In the low-temperature phase there is clear evidence of parallel displacements of the cations away from the centres of their anion polyhedra, indicative of ferroelectric behaviour. The implications of this finding for the wider topic of structural systematics within perovskite-structured compounds are briefly discussed.

1. Introduction

Of all the crystal structures adopted by inorganic compounds, the perovskite arrangement observed in systems with stoichiometry ABX_3 is arguably one of the most important. Compounds with this ionic arrangement, or derivatives of it, have been widely studied owing to diverse potential technological applications, which are linked to ferroelectric [1], magnetoresistive [2], high-T_c superconducting [3] and ionic conducting [4] properties. As

[4] Author to whom any correspondence should be addressed. Telephone: +44 1235 446628; fax: +44 1235 445720.

illustrated in figure 1, the 'ideal' cubic perovskite structure is very simple, with the A and B cations in the 1(b) $\frac{1}{2}, \frac{1}{2}, \frac{1}{2}$ and 1(a) $0, 0, 0$ sites of space group $Pm\bar{3}m$, respectively, and the X anions in the 3(c) positions at $\frac{1}{2}, 0, 0$ etc. The larger A cations are surrounded by twelve anions which form an cuboctahedron, whilst the smaller B species lie at the centre of an octahedron of anions. The crystal structure is then a three-dimensional network of corner-sharing BX_6 octahedra with the A cations sitting at the centre of a cube formed by eight octahedra. However, as noted by Hyde and Andersson [5], this structure is 'overdetermined' because the only degree of freedom is the cubic unit-cell constant a and, in the hard-sphere model of ionic contacts, it is necessary to simultaneously satisfy the conditions $r_A + r_X = a/\sqrt{2}$ and $r_B + r_X = a/2$, where r_i is the ionic radius of ion i. These requirements are combined in the so-called 'Goldschmidt tolerance factor' $t_G = (r_A + r_X)/\sqrt{2}(r_B + r_X)$ [6], which, in the ideal case, equals unity. In reality, perovskite-structured compounds are found to adopt the cubic arrangement for $0.97 \lesssim t_G \lesssim 1.03$ [7]. For larger values of t_G hexagonal structures are preferred, in which there is some degree of edge sharing of the BX_6 octahedra [5], whilst for lower t_G-values there are a number of possibilities, including a correlated tilting of the BX_6 octahedra, distortions of the octahedral units and cooperative displacements of the B cations away from the centres of the octahedra.

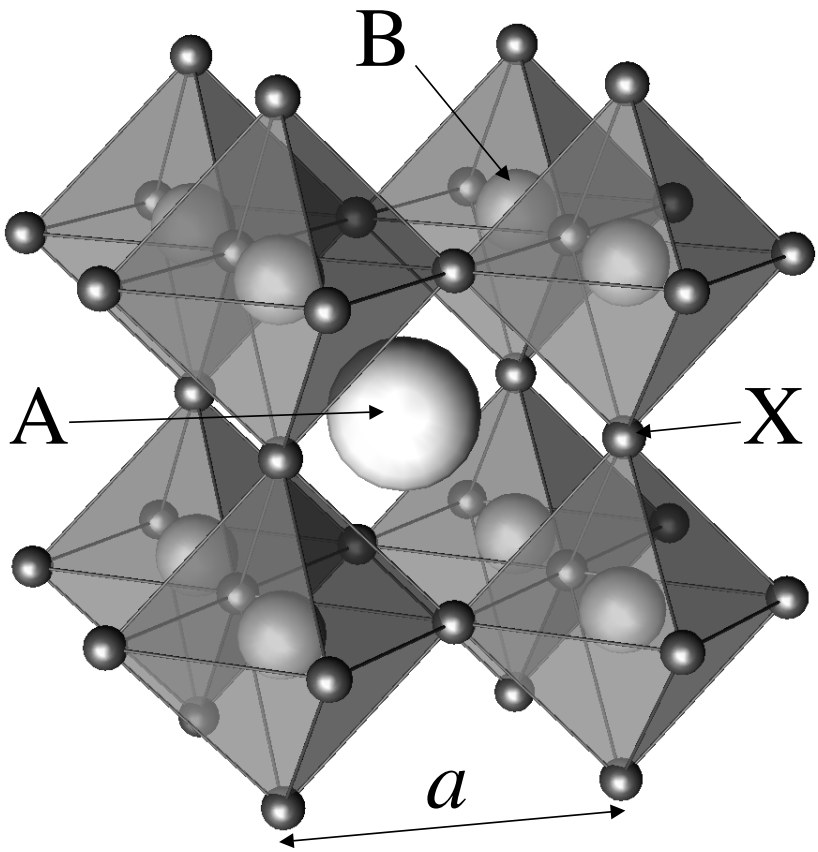

Figure 1. The ideal cubic perovskite structure of an ABX_3 compound, showing the larger A cation sitting at the centre of a cube of eight corner-sharing BX_6 octahedra, The cubic lattice parameter a is illustrated.

Systematic studies of the nature of the structural distortions within perovskites [7–14] have largely concentrated on oxide ABO_3 compounds, since these are more numerous and the most relevant from the technological point of view. In comparison, the fluoride ABF_3 compounds are less well understood, even though they can be used as 'model' systems for studying the structural and physical properties of oxide perovskites under temperatures and pressures which are difficult to attain experimentally. As an example, the fluoride perovskite $NaMgF_3$ has been widely studied [15–17] because it is isoelectronic and isostructural to $MgSiO_3$, which is an important component of the Earth's lower mantle [18]. In addition, fluoride analogues of the ferroelectric oxides $BaTiO_3$ and $Pb(Zr_{1-x}Ti_x)O_3$ (PZT) are desirable, since these may have promising dielectric properties for capacitor applications [19]. In this article we describe an impedance spectroscopy and powder neutron diffraction study of the perovskite-related compound $CsPbF_3$ below room temperature.

2. Experimental procedure

The polycrystalline sample of $CsPbF_3$ was prepared by mixing stoichiometric amounts of CsF and PbF_2 in a nitrogen-filled dry box. The reactants had previously been dried overnight at 425(5) K in a vacuum oven. The samples were pelletized and then dried at 475(5) K for 2 h to remove any traces of moisture before sintering at 700(3) K for 15 h in a gold tube under dynamic vacuum. Two-terminal measurements of the ionic conductivity were performed using a pelleted sample of ∼6 mm diameter and ∼6 mm length over the temperature range $150 \lesssim T\ (\mathrm{K}) \lesssim 300$ in steps of approximately 6 K. The sample was held between spring-loaded platinum contacts in a specially designed cell attached to a closed-cycle refrigerator. Details of this device can be found elsewhere [20]. A PC-controlled Solartron S1260 Frequency Response Analyser determined the conventional Z–Z' impedance plot over the frequency range from 0.1 Hz to 10 MHz. The real component of the sample impedance Z_S was determined using the program IMMFIT [20]. The powder diffraction experiments were performed on the High Resolution Powder Diffractometer (HRPD) at the ISIS facility, UK [21], with ∼6 g of sample encapsulated inside a thin-walled vanadium cylindrical can. Diffraction data were collected using the backscattering detector bank which provides data over the d-spacing range $0.3 < d\ (\text{Å}) < 2.1$ with a resolution $\Delta d/d \sim 5 \times 10^{-4}$. Indexing of the measured d-spacings used the program TREOR-90 [22] and Rietveld profile refinements of the normalized diffraction data were performed using the program TF12LS [23], which is based on the Cambridge Crystallographic Subroutine Library [24].

3. Results

The variation of the ionic conductivity σ of $CsPbF_3$ with temperature is illustrated in figure 2. At temperatures close to ambient, σ is moderately high ($\sim 10^{-4}\ \Omega^{-1}\ \mathrm{cm}^{-1}$), suggesting that the F^- are relatively mobile. The nature of this disorder within PbF_2–MF, $M = K^+$, Rb^+ and Cs^+, systems at elevated temperatures has been reported elsewhere [25, 26]. On cooling, there is no evidence of a discontinuity in σ versus T for $CsPbF_3$, though a change of the slope $\mathrm{d}\sigma/\mathrm{d}T$ occurs at 185(2) K. This supports the report of a structural phase transition at ∼190 K on the basis of NMR studies [27].

A preliminary measurement of the diffraction pattern at ambient temperature confirmed the sample to be a cubic perovskite ($Pm\bar{3}m$) with $a = 4.800\,32(1)$ Å. To investigate the structural nature of the transition at $T \sim 190$ K the sample was cooled at ∼20 K h^{-1} to 148 K and held at this temperature (±5 K) for approximately 10 h prior to measurements. A relatively

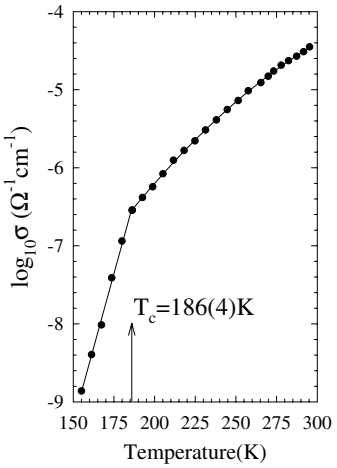

Figure 2. The variation of the ionic conductivity σ of $CsPbF_3$ showing the change in slope $d\sigma/dT$ at the phase transition temperature $T = 186(4)$ K.

long data collection (∼6 h) was performed at this temperature, in order to collect diffraction data of sufficient statistical quality for structure solution and refinement. The sample was then heated and data collected for ∼2 h at eleven temperatures in the range $148 \leqslant T$ (K) $\leqslant 276$. In all cases the temperature stability was better than ±2 K during the period of data collection. A portion of the diffraction data collected on heating are illustrated in figure 3. There is clear evidence of a structural transition at ∼187(5) K, in which several of the peaks of the cubic

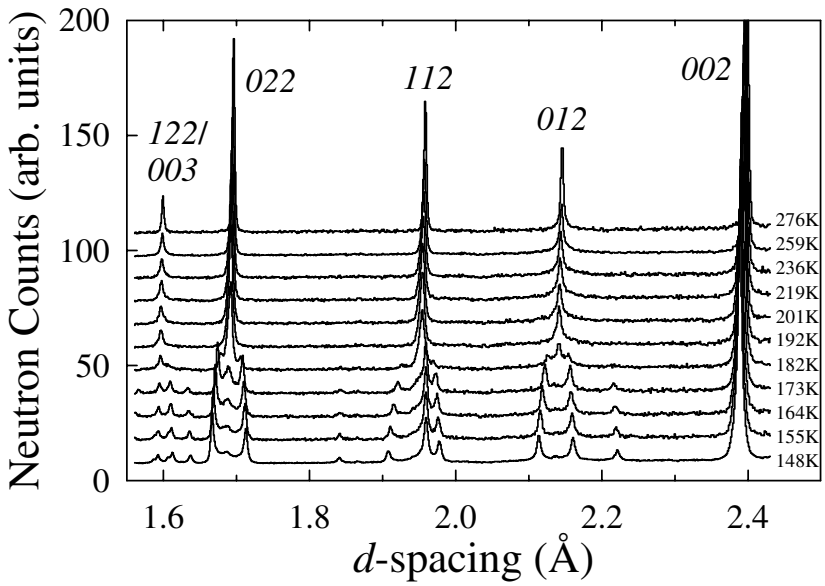

Figure 3. Evolution of the neutron diffraction pattern collected from $CsPbF_3$ at eleven temperatures in the range $148(2) \leqslant T$ (K) $\leqslant 276(2)$. The cubic → rhombohedral phase transition at $T = 187(5)$ K is clearly visible. The *hkl* indices of the cubic phase are shown.

($Pm\bar{3}m$) perovskite phase become split and additional weak reflections appear. The majority of the d-spacings observed in the data collected at 148(2) K could be indexed on the basis of a hexagonal unit cell with $a \approx 6.85$ Å and $c \approx 16.12$ Å. However, as shown in table 1, a small number of additional peaks were observed and identified as arising from a small fraction of remaining cubic phase. The ratio of the volumes of the unit cells of the hexagonal and cubic modifications indicates that the former contains six formula units. Furthermore, the indices of the reflections for the hexagonal unit cell all satisfy $-h+k+l = 3n$, indicating rhombohedral symmetry. We therefore label the high-temperature cubic and low-temperature rhombohedral phases c-$CsPbF_3$ and rh-$CsPbF_3$, respectively.

Table 1. The d-spacings of the reflections in the range $1.5 < d(\text{Å}) < 3.5$ observed for $CsPbF_3$ at $T = 148(2)$ K. The calculated positions of the peaks from the rhombohedral rh-$CsPbF_3$ ($R3c$) and cubic c-$CsPbF_3$ ($Pm\bar{3}m$) phases are listed, together with their hkl indices.

Measured	rh-$CsPbF_3$ ($R3c$) $a = 6.849\,93(6)$ Å, $c = 16.1205(1)$ Å		c-$CsPbF_3$ ($Pm\bar{3}m$) $a = 4.7748(2)$ Å	
d_{obs} (Å)	d_{calc} (Å)	hkl	d_{calc} (Å)	hkl
3.425	3.425	$2\bar{1}0$		
3.371			3.375	011
3.335	3.334	104		
2.888	2.888	$2\bar{1}3$		
2.784	2.783	202		
2.686	2.687	006		
2.389	2.389	$20\bar{4}$	2.387	002
2.221	2.221	$3\bar{1}1$		
2.161	2.160	$3\bar{1}\bar{2}$		
2.114	2.114	$2\bar{1}6$		
1.977	1.977	300		
1.959	1.959	$3\bar{1}4$		
1.908	1.908	$10\bar{8}$		
1.840	1.841	$3\bar{1}\bar{5}$		
1.712	1.712	$4\bar{2}0$		
1.686			1.688	022
1.666	1.667	208		
1.637	1.637	$4\bar{1}\bar{1}$		
1.612	1.612	$4\bar{1}2$		
1.606	1.607	$3\bar{1}7$		
1.592	1.593	306	1.591	122/003
1.586	1.587	$2\bar{1}9$		
1.555	1.556	1 0 10		
1.523	1.523	$4\bar{1}\bar{4}$		

There are seven rhombohedral space groups, $R3$, $R\bar{3}$, $R32$, $R3m$, $R\bar{3}m$, $R3c$ and $R\bar{3}c$. In principle, the latter two can be distinguished from the rest on the basis of the observed reflection conditions [28]. However, several of the peaks arising from the distortions from the cubic aristotype structure are inherently weak and it is not wholly reliable to assign a space group according to the presence (or absence) of a small number of weak reflections, especially in the presence of a second minority phase. We therefore adopt the most general approach and attempt to fit the data using each space group in turn. One exception is $R\bar{3}$, since it cannot be used to describe a perovskite-type arrangement which retains connectivity of the octahedra as they are rotated or distorted [10]. In the case of $R\bar{3}m$, the only deformation allowed is the

flattening or elongation of the octahedra along the threefold axis if the axial ratio c/a differs from the ideal value of $\sqrt{6}$. In space groups $R3c$, $R3m$ and $R3$ the octahedra may additionally distort in a manner which retains the threefold axis but allows the sizes of the two triangular faces of the octahedra above and below the B cation along the c-axis to differ in size. Rotation of the anions about the threefold axis is allowed in space groups $R3$, $R32$, $R3c$ and $R\bar{3}c$. In the first two cases the faces above and below the B cation rotate in opposite directions and the octahedra become heavily distorted whilst in the latter two space groups the two faces rotate in the same direction and the octahedra tilts as a rigid unit. Finally, in the polar space groups $R3$, $R3m$ and $R3c$ the cations are allowed to independently shift up and down the threefold axis away from the centres of their polyhedra.

In assessing the relative quality of fits to the experimental data using different structural models, the usual χ^2 statistic is used, defined by

$$\chi^2 = \sum_{N_d} \frac{(I_{obs} - I_{calc})^2}{(\sigma I_{obs})^2} \Big/ (N_d - N_p).$$

N_d is the number of data points used in the fit and N_p is the number of fitted parameters. I_{obs} and I_{calc} are the observed and calculated intensities, respectively, and σI_{obs} is the estimated standard deviation on I_{obs}, derived from the counting statistics. The values of χ^2 obtained by fitting each model are summarized in table 2. A good fit is achieved using space group $R\bar{3}c$, though a significant improvement in χ^2 is obtained by lowering the symmetry to $R3c$. The values of the structural parameters obtained by fitting the data using this model are listed in table 3 and the quality of the fit to the experimental data is illustrated in figure 4. The extent of the structural distortions within the low-temperature rh-$CsPbF_3$ phase is illustrated in figure 5. The rotation of the PbF_6 octahedra in rh-$CsPbF_3$ is relatively modest ($\omega \sim 9^\circ$) and, as a consequence, the coordination around the Cs^+ is still essentially twelvefold, with Cs^+–F^-

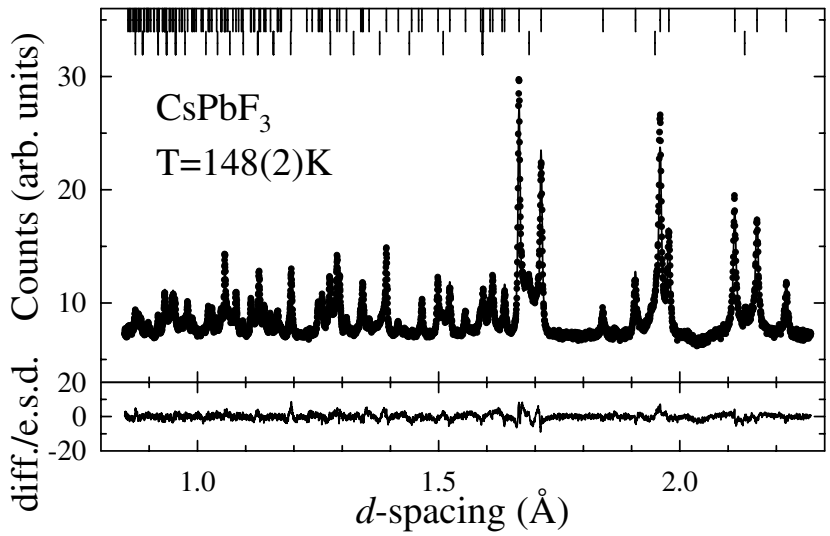

Figure 4. Time-of-flight least-squares refinement of the neutron diffraction data collected from $CsPbF_3$ at $T = 148(2)$ K. The dots are the experimental data points and the solid line is the calculated profile, with the parameters listed in table 3. The lower trace is the difference (observed minus calculated) divided by the estimated standard deviation on the experimental data points. The tick marks denote the calculated positions of the reflections from the rhombohedral rh-$CsPbF_3$ (upper) and cubic c-$CsPbF_3$ (lower) phases.

Table 2. The values of the goodness-of-fit statistic χ^2 obtained by fitting the diffraction data collected from $CsPbF_3$ at $T = 148(2)$ K using the six possible rhombohedral space groups. * denotes that the fit failed to converge satisfactorily due to excessive shifts in the positional parameters.

Rhombohedral space group	χ^2
$R3$ (No 146)	8.53
$R32$ (No 155)	9.37
$R3m$ (No 160)	~ 11*
$R3c$ (No 161)	2.92
$R\bar{3}m$ (No 166)	11.30
$R\bar{3}c$ (No 167)	4.54

Table 3. The parameters obtained by fitting the diffraction data collected from $CsPbF_3$ at $T = 148(2)$ K.

Phase	rh-$CsPbF_3$	c-$CsPbF_3$
Temperature	$T = 148(2)$ K	
Volume fraction	$V_{rh} = 91.4(1)\%$	$V_c = 8.6(1)\%$
Space group	$R3c$	$Pm\bar{3}m$
Lattice parameters	$a = 6.84993(6)$ Å $c = 16.1205(1)$ Å	$a = 4.7748(2)$ Å
Unit-cell volume	$V = 655.063(7)$ Å^3	$V = 108.864(5)$ Å^3
Volume per formula unit	$V/Z = 109.177(2)$ Å^3	$V/Z = 108.864(5)$ Å^3
Ionic positions	Cs^+ in 6(a) 0, 0, z_{Cs} $z_{Cs} = 0.2428(5)$ Pb^{2+} in 6(a) 0, 0, z_{Pb} $z_{Pb} = -0.0076(3)$ F^- in 18(b) x_F, y_F, z_F $x_F = 0.5319(3)$ $y_F = -0.0327(4)$ $z_F = 1/4$ (to fix origin)	Cs^+ in 1(b) at 1/2, 1/2, 1/2 Pb^{2+} in 1(a) at 0, 0, 0 F^- in 3(c) at 1/2, 0, 0
Thermal parameters	$B_{Cs} = 0.85(6)$ Å^2 $B_{Pb} = 0.45(4)$ Å^2 $B_F = 2.04(5)$ Å^2	$B_{Cs} = 0.7(1)$ Å^2 $B_{Pb} = 0.6(1)$ Å^2 $B_F = 1.4(2)$ Å^2
No of data points	$N_d = 4703$	
No of profile parameters	$N_p = 7$	
No of structural parameters	$N_p = 9$	$N_p = 4$
Goodness of fit	$\chi^2 = 2.92$	
Weighted R-factor	$R_w = 3.45\%$	
Expected R-factor	$R_{exp} = 2.02\%$	

distances of 3.10(1) Å (×3), 3.14(1)Å (×3), 3.56(1)Å (×3) and 3.76(1)Å (×3). The most distinctive structural feature of rh-$CsPbF_3$ is the c/a ratio (2.353 38(2)) being significantly lower than its ideal value of $\sqrt{6} = 2.449\,49$. This corresponds to a marked flattening of the PbF_6 octahedra along the c-axis, such that there are four different F^-–F^- distances of 3.141(6)Å (×3), 3.336(8)Å (×3), 3.402(8)Å (×3) and 3.805(9)Å (×3). The displacements of the Cs^+ and Pb^{2+} away from the centres of their polyhedra along the c-axis are 0.116(8)Å and 0.123(5)Å, respectively.

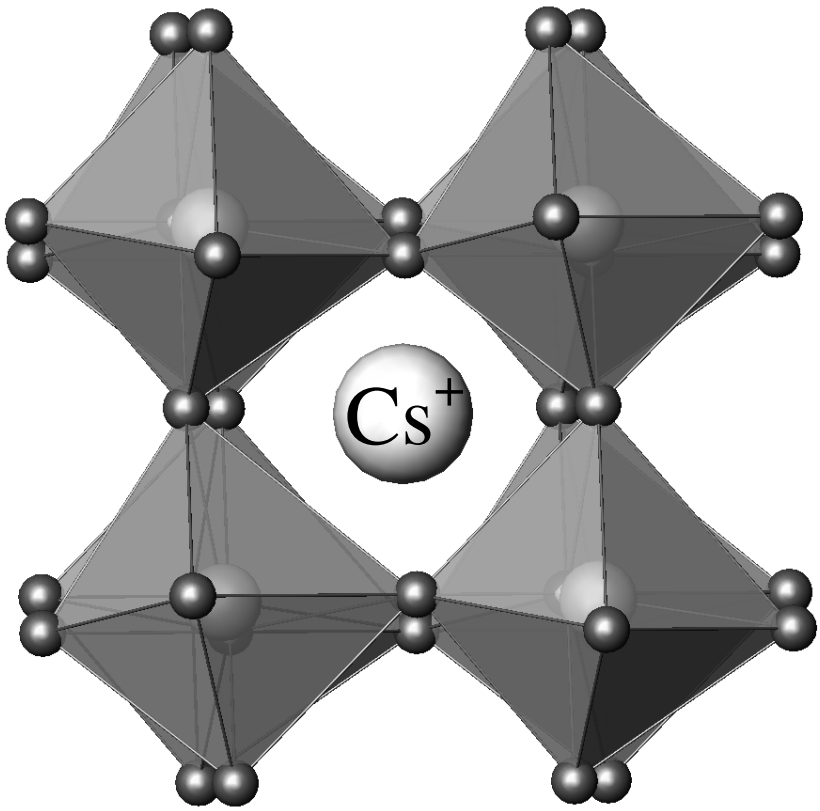

Figure 5. The structure of the low-temperature rhombohedral phase of rh-$CsPbF_3$ at $T = 148(2)$ K, showing the rotation of the PbF_6 octahedra.

4. Discussion

For the perovskite structure, Glazer [9] has considered the tilting of essentially rigid BX_6 octahedra about the three cubic axes, identified 23 possible tilt systems and derived their space groups. These assignments were confirmed with only minor corrections by Woodward [13], who also show that in 6 of the tilt systems it was necessary to allow small distortions of the octahedra in order to retain connectivity. Recently, Howard and Stokes [14] have addressed the same problem using group theoretical methods and conclude that 8 of the original 23 tilt systems can be discounted on physical grounds because they have a higher symmetry than required by their space group (i.e. the tilts around two different axes are constrained to be of equal magnitude even though there is no physical reason for them to be so). The remaining 15 tilt systems were shown to account for all the reliable published structural data on perovskite-like compounds [7]. In addition, a recent compilation of the structural data for such systems indicates a strong preference for those space groups in which all the A cations are on a single set of symmetry-equivalent positions [7]. Of the seven tilt systems which meet this requirement, the majority of compounds are found to adopt the undistorted cubic $Pm\bar{3}m$ structure for $t_G \sim 1$ and rhombohedral ($R\bar{3}c$) and orthorhombic ($Pnma$) variants as the magnitude of the tilts increases (i.e. t_G decreases). Lattice energy calculations [7] show that the orthorhombic and rhombohedral variants are comparable, though increased ion–ion repulsions

destabilize the latter with respect to the former as the tilt angle increases. In addition, there is a contribution to the stability of the rhombohedral distortion due to Coulomb terms which decrease as the charge of the A cations decreases. If the latter argument is applied to fluoride perovskites (with monovalent A cations), then one would not expect any ABF_3 rhombohedral compounds. A search of the current literature (using the Inorganic Crystal Structure Database (ICSD)) supports this expectation, with 29 fluoride compounds known in $Pm\bar{3}m$ symmetry, 12 in $Pnma$ symmetry but none in any of the rhombohedral space groups discussed above. Therefore, to the best of our knowledge, $CsPbF_3$ is the first example of a rhombohedrally distorted fluoride perovskite.

In general terms, the greater degree of ionicity of the fluorine bond favours high-symmetry coordinations and so hinders the formation of small off-centre cation displacements which characterize ferroelectric behaviour. Indeed, a recent review by Ravez [19] concluded that the number of ferroelectric fluorides is significantly smaller than the number of oxides, with only six families of compounds of stoichiometries $A_2^+B^{2+}F_4$, $A^{2+}B^{2+}F_4$, $A^{2+}B^{3+}F_5$, $A_2^+B^{2+}C^{3+}F_7$, $A_3^+B_3^{2+}C_2^{3+}F_{15}$ and $A_5^{2+}B_3^{3+}F_{19}$. Clearly, the significantly better fit obtained using $R3c$ symmetry over $R\bar{3}c$ indicates the presence of cation displacements in rh-$CsPbF_3$. Confirmation of ferroelectric behaviour requires the measurement of dielectric properties. However, attempts to measure the polarizability within the low-temperature rhombohedral phase proved unsuccessful, due to the high ionic conductivity of the sample (figure 2). Similar difficulties have been reported in the case of Ag_3SI [29] (which undergoes a rhombohedral distortion of its cubic anti-perovskite structure in space group $R3$ [30] on cooling below 156 K) due to the high mobility of the Ag^+. However, we note that the structural description given in table 3 meets the structural criteria for ferroelectric behaviour given by Abrahams [31], though Ravez [19] found no evidence of ferroelectric fluorides with stoichiometry $A^+B^{2+}F_3$. Again, $CsPbF_3$ appears unique. This is consistent with the structural preference for orthorhombic rather than rhombohedral distortion in fluoride perovskites discussed above and the conclusions of Thomas [12] that orthorhombic perovskites have the capability of showing the appropriate cation displacements to display ferroelectric properties, but this is rarely the case in practice. Instead, the nature of the tilts in the rhombohedral distortion requires the B-ion displacements to be parallel and thus more likely to lead to an overall spontaneous polarization. However, contrary to these remarks, calculations of the lattice energies of numerous ABF_3 compounds (A = Li, Na, K, Rb, Cs; B = Mg, Ca, Sr, Ba) have predicted a transition to a low-temperature rhombohedrally distorted ferroelectric phase in several compounds [32, 33], though these compounds do not exist due to the preferential formation of other phases of different stoichiometries.

Overall, the structural behaviour of $CsPbF_3$ is most similar to that of $CsGeCl_3$, $CsGeBr_3$ and $CsGeI_3$ [34], which all undergo transitions from cubic to rhombohedral symmetry at temperatures of 428 K, 511 K and 550 K, respectively [34]. The low-temperature forms all adopt space group $R3m$ and thus differ from $CsPbF_3$ by the absence of any rotation of the octahedra about the threefold axis (i.e. $\omega = 0$). However, they are reported to be ferroelectric [35] and the ionic conductivity of $CsGeCl_3$ at the phase transition shows similar behaviour to $CsPbF_3$, with no discontinuity in σ [36]. Interestingly, $CsPbF_3$ differs from $CsPbCl_3$ [37] and $CsPbBr_3$ [38], both of which are cubic perovskite ($Pm\bar{3}m$) structured above 403 K and 320 K, respectively, but undergo several phase transitions at lower temperatures to phases with orthorhombic, tetragonal and monoclinic symmetries [37, 38].

Finally, we turn our attention to the nature of the low-temperature phase transition in $CsPbF_3$. In principle, this can be a continuous transition, as observed in the case of the second-order $R\bar{3}c \rightarrow Pm\bar{3}m$ transition studied recently in $LaAlO_3$ at 820 K [39]. For the case of the $R3c \rightarrow Pm\bar{3}m$ transition within $CsPbF_3$, this would require $c/a \rightarrow \sqrt{6}$, $z_{Cs} \rightarrow 1/4$,

$z_{Pb} \rightarrow 0$, $x_F \rightarrow 1/2$ and $y_F \rightarrow 0$, such that the octahedral rotation angle $\omega \rightarrow 0^\circ$. Indeed, the behaviour of the ionic conductivity (figure 2) implies that the transition in $CsPbF_3$ is continuous. However, as illustrated for c/a and ω in figure 6, this is not the case in $CsPbF_3$ and there is a clear discontinuity in the structural behaviour at the transition temperature. Subsequent measurements in which the sample was cooled more rapidly ($\sim$3 K min^{-1}) from room temperature to $T = 2.3(5)$ K gave a diffraction pattern consistent with the rhombohedral structure (see figure 7) but with extremely broad reflections. This is consistent with the formation of small rhombohedral domains. This observation, together with the coexistence of

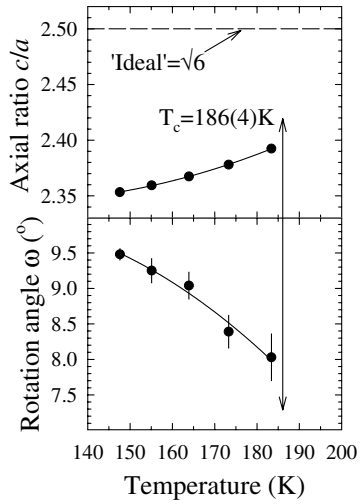

Figure 6. The variation with temperature of the unit-cell parameter ratio c/a and the angle ω describing the tilt of the PbF_6 octahedra about the pseudocubic axis.

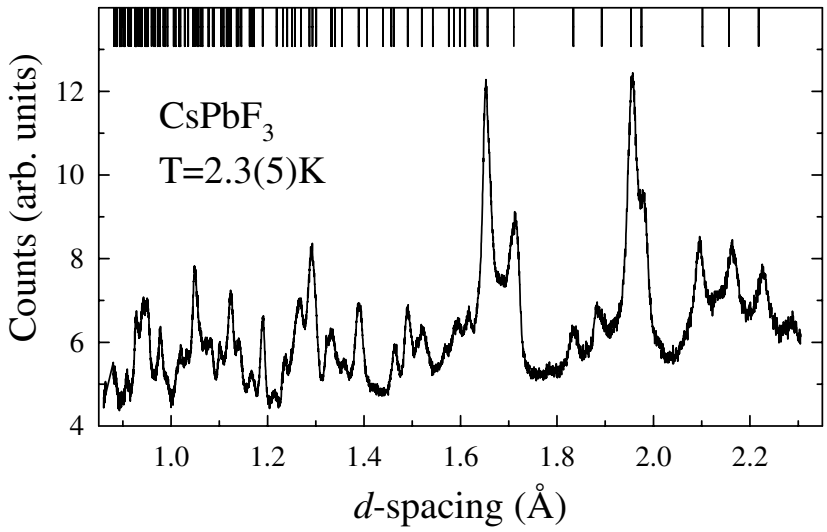

Figure 7. A portion of the neutron diffraction pattern collected from rh-$CsPbF_3$ at $T = 2.3(5)$ K. The tick marks denote the calculated positions of the reflections from a rhombohedral unit cell (with $a \sim 6.842$ Å and $c = 15.976$ Å).

rhombohedral and cubic phases at temperatures close to the transition, indicates that kinetic effects play a significant role in the formation of the rh-$CsPbF_3$ phase and will require more detailed future studies.

5. Conclusions

The above discussion illustrates the unique nature of the low-temperature phase of $CsPbF_3$, where the off-centre displacements presumably arise due to the electronic structure of Pb^{2+}. The structural characterization of the cubic-to-rhombohedral phase transition at $T = 186(4)$ K reported in this paper forms the motivation for further studies of its dielectric properties and the nature of its bonding character.

Acknowledgments

One of the authors (PB) wishes to thank the Swedish Foundation for International Cooperation in Research and Higher Education for financial support. We are grateful to R M Ibberson for his assistance with the neutron diffraction studies and to N J G Gardner for the development of the complex impedance spectroscopy apparatus.

References

[1] Shirane G, Danner H and Pepinski R 1957 *Phys. Rev.* **105** 856
[2] Hwang H Y, Cheong S-W, Radaelli P G, Marezio M and Batlogg B 1995 *Phys. Rev. Lett.* **75** 914
[3] Cava R J, van Dover R B, Batlogg B and Rietman E A 1987 *Phys. Rev. Lett.* **58** 408
[4] Nowick A S and Du Y 1995 *Solid State Ion.* **77** 137
[5] Hyde B G and Andersson S 1989 *Inorganic Crystal Structures* (New York: Wiley-Interscience)
[6] Goldschmidt V M 1926 *Naturwissenschaften* **14** 477
[7] Woodward P M 1997 *Acta Crystallogr.* B **53** 44
[8] Michel C, Moreau J M and James W J 1971 *Acta Crystallogr.* B **27** 501
[9] Glazer A M 1972 *Acta Crystallogr.* B **28** 3384
[10] Megaw H D and Darlington C N W 1975 *Acta Crystallogr.* A **31** 161
[11] Thomas N W and Beitollahi A 1994 *Acta Crystallogr.* B **50** 549
[12] Thomas N W 1996 *Acta Crystallogr.* B **52** 16
[13] Woodward P M 1997 *Acta Crystallogr.* B **53** 32
[14] Howard C J and Stokes H T 1998 *Acta Crystallogr.* B **54** 782
[15] Andersen N H, Kjems J K and Hayes W 1985 *Solid State Ion.* **17** 143
[16] Zhou L X, Hardy J R and Cao H Z 1997 *Geophys. Res. Lett.* **24** 747
[17] Street J N, Wood I G, Knight K S and Price G D 1997 *J. Phys.: Condens. Matter* **9** L647
[18] O'Keeffe M and Bovin J-O 1979 *Science* **206** 599
[19] Ravez J 1997 *J. Physique* III **7** 1129
[20] Gardner N J G, Hull S, Keen D A and Berastegui P 1998 *Rutherford Appleton Laboratory Report* RAL-TR-1998-032
[21] Ibberson R M, David W I F and Knight K S 1992 *Rutherford Appleton Laboratory Report* RAL-92-031
[22] Werner P-E, Eriksson L and Westdahl M 1985 *J. Appl. Crystallogr.* **18** 367
[23] David W I F, Ibberson R M and Matthewman J C 1992 *Rutherford Appleton Laboratory Report* RAL-92-032
[24] Brown P J and Matthewman J C 1987 *Rutherford Appleton Laboratory Report* RAL-87-010
[25] Hull S, Berastegui P, Eriksson S G and Gardner N J G 1998 *J. Phys.: Condens. Matter* **10** 8429
[26] Hull S and Berastegui P 1999 *J. Phys.: Condens. Matter* **11** 5257
[27] Bouznik V M, Moskvich Yu N and Voronov V N 1976 *Chem. Phys. Lett.* **37** 464
[28] *International Tables for Crystallograllography* 1996 vol A, ed T Hahn (Dordrecht: Kluwer)
[29] Hoshino S, Fujishita H, Takashige M and Sakuma T 1981 *Solid State Ion.* **3+4** 35
[30] Hull S, Keen D A, Gardner N J G and Hayes W 2001 *J. Phys.: Condens. Matter* **13** 2295
[31] Abrahams S C 1988 *Acta Crystallogr.* B **44** 585

[32] Edwardson P J, Boyer L L, Newman R L, Fox D H, Hardy J R, Flocken J W, Guenther R A and Mei W 1989 *Phys. Rev.* B **39** 9738
[33] Allan N L, Dayer M J, Kulp D T and Mackrodt W C 1991 *J. Mater. Chem.* **1** 1035
[34] Thiele G, Rotter H W and Schmidt K D 1987 *Z. Anorg. Allg. Chem.* **545** 148
[35] Christensen A N and Rasmussen S E 1965 *Acta Chem. Scand.* **19** 421
[36] Yamada K, Isobe K, Okuda T and Furukawa Y 1994 *Z. Naturf.* a **49** 258
[37] Fujii Y, Hoshino S, Yamada Y and Shirane G 1974 *Phys. Rev.* B **9** 4549
[38] Sharma S, Weiden N and Weiss A 1991 *Z. Naturf.* a **46** 329
[39] Howard C J, Kennedy B J and Chakoumakos B C 2000 *J. Phys.: Condens. Matter* **12** 349